SUPPLEMENTARY INFORMATION FOR:

eIF4B preferentially stimulates translation of long mRNAs with structured 5'UTRs and low closed-loop potential but weak dependence on eIF4G

Inventory:

Supplemental Methods

Additional File 1

Supplementary Figures 1-8

SUPPLEMENTAL METHODS

Plasmid Constructions

Plasmid pFJZ526, containing the *FLUC* reporter with synthetic unstructured 5'UTR (Fig. S8), was constructed by the following steps. A PCR product was amplified from pFJZ450 (1) with primer pair FZ219/218 and used as template for a second PCR amplification with primers FZ220/218. The resulting PCR product was cloned between the EcoRI and SalI sites of PBluescript II KS+ to generate intermediate plasmid pFJZ489. The *RPL41A* promoter was PCR-amplified from pFJZ254 (1) with primers FZ160/FZ223 and inserted between the NotI/EcoRI sites of pFJZ489 to generate a second intermediate, pFJZ491. Subsequently, the SacI-SalI fragment containing the *RPL41A* promoter, artificial 5'UTR, *FLUC* CDS, and shortened *RPL41A* 3'UTR with 3' flanking sequences was isolated from pFJZ491 and cloned between the SacI/SalI sites in YCplac33 to generate pFJZ526.

Derivatives of pFJZ526 harboring cap-proximal SL insertions in the 5'UTR of the *FLUC* reporter, pFJZ683 and pFJZ685 (Fig. S8), were produced as follows. pFJZ491 was digested at the EcoRI site in the 5'UTR and re-ligated in the presence of oligonucleotide pairs FZ377/378 or FZ381/382 to generate pFJZ497 and pFJZ642, respectively, containing cap-proximal SL insertions of ΔG = -10.5 kcal/mol (pFJZ497) and ΔG = -8.1 kcal/mol (pFJZ642). The SacI-SalI fragments containing the complete *FLUC* reporter genes in pFJZ497 and pFJZ642 were cloned between the same sites in YCplac33 to generate plasmids pFJZ683 and pFJZ685, respectively.

Derivatives of pFJZ526 harboring cap-distal SL insertions, pFJZ688 and pFJZ690 (Fig. S8) were produced as follows, beginning with construction of the intermediate plasmid pFJZ490. A PCR product was amplified from pFJZ450 (1) with primers FZ221/218 , digested with EcoRI

and SalI and cloned between the same sites in PBluescript II KS+ to generate pFJZ490. The *RPL41A* promoter was PCR-amplified from pFJZ254 (1) with primers FZ160/FZ223 and inserted between the NotI/EcoRI sites of pFJZ490 to generate a second intermediate, pFJZ492. pFJZ492 was digested with EcoRI in the 5'UTR and re-ligated in the presence of oligonucleotide pairs, FZ377/378 or FZ381/383 to generate cap-distal SL constructs pFJZ645 (ΔG = -10.5 kcal/mol) and pFJZ647 (ΔG = -8.1 kcal/mol), respectively. The SacI-SalI fragments containing the complete *FLUC* reporter genes in pFJZ645 and pFJZ647 were isolated and cloned between the same sites in YCplac33 to generate plasmids pFJZ688 and pFJZ690, respectively.

Plasmids pFJZ538 and pFJZ541 used to assay reporter mRNA association with native 40S subunits were generated in the following steps. The *RPL41A* shortened 3'UTR was amplified from plasmid pFJZ335 (1) with primers FZ227/FZ70. An XmaI site and *FLUC* codons 2-18 were embedded in the forward primer FZ277. The resulting PCR product was digested with XmaI/SalI, and cloned between the same sites in pFJZ491 and pFJZ497, replacing the full-length *FLUC* CDS with only the N-terminal 51nt of *FLUC* CDS in the resulting intermediate constructs pFJZ515 and pFJZ518, respectively. The complete reporter genes containing *RPL41A* promoter, artificial leader, 17 *FLUC* codons and shortened *RPL41A* 3'UTR in pFJZ515 and pFJZ518 were isolated on SacI/SalI fragments and cloned between the same sites in YCplac33, to generate plasmids pFJZ538 and pFJZ541, respectively.

Sequences of primers described above are as follows (listed 5' to 3'): FZ70 (AAA GTC GAC GAT ATA TGT AGC ATT TAT CTT CTG); FZ160 (CCC AGA TCT GCG GCC GCT GTA GAT TGT CCA CTA TCT CAT G); FZ218 (CCC GTC GAC TTT TCA AAA AAA CGG ACA ATT GAT TAA ACT ATG TGA GAC ATA TAT AAA GCA CTA TAT AAA GGA TCC TGG TCG GGT GTA GA); FZ219 (ATG CAC CAC CAC CAC CAC CAC CCC GGG GAA

GAC GCC AAA AAC ATA AAG AAA); FZ220 (CCC GAA TTC AAC AAC AAC AAC AAC AAC AAC AAC AAC AAC AAC AAC AAC AAC AAC AAC AAC AAC AAC AAC AAA AAA TGC ACC ACC ACC ACC ACC AC); FZ221 (CAA GAA TTC CAA CAA CAA CAA CAA AAA ATG CAC CAC CAC CAC CAC CAC CCC GGG GAA GAC GCC AAA AAC ATA AAG AAA); FZ223 (GGG GAA TTC TTG TTG TTG TTG TTG TTG TTG TTG TTG TTG TTG TTG TTG GGT CTG GTT CTT TTA GTA CAA AAT GGA AC); FZ227 (CGC CCC GGG GAA GAC GCC AAA AAC ATA AAG AAA GGC CCG GCG CCA TTC TAT CCT CTA TAA GCG GAT CTA AAT TGC ATA CTA ATC); FZ377 (AAT TGC CAT CTT GGC); FZ378 (AAT TGC CAA GAT GGC); FZ381 (AAT TAT CAT CTT GGT); FZ382 (AAT TAC CAA GAT GAT); FZ383 (AAT TTC CAT CTT GGC).

Polysome profile analysis and quantification of reporter mRNA association with native 40S subunits

For polysome profile analysis, strains were cultured under the conditions specified in Fig. S1, cycloheximide was added to 50μg/mL for 5min prior to harvesting, and WCEs were prepared and resolved by sedimentation through sucrose density gradients. WCEs were prepared by vortexing the cell pellet with glass beads in cold breaking buffer (20 mM Tris-HCl [pH 7.5], 50 mM NaCl, 10 mM $MgCl_2$, 1 mM DTT, 200 μg/mL heparin, 50 μg/mL cycloheximide, and 1 Complete EDTA-free Protease Inhibitor cocktail Tablet [Roche]/50 mL buffer). 12.5 A_{260} units of WCEs were separated by velocity sedimentation on a 4.5%–45% sucrose gradient by centrifugation at 39,000 rpm for 3.1h at 4°C in a SW41Ti rotor (Beckman), and gradient fractions were scanned at 254 nm to visualize ribosomal species.

To measure association of reporter mRNAs with native 40S subunits, cells were cross-linked with 2% HCHO for 1h prior to harvesting as described (2). Twenty-five A_{260} units of WCEs were resolved by sedimentation through 7.5- 30% sucrose gradients by centrifugation at 41,000 rpm for 4.5h. Gradient fractions were scanned at 254 nm and collected. Purification of total RNA from gradient fractions and qRT-PCR analysis of mRNA abundance was conducted as described (2).

Generation, processing, and analysis of sequence libraries of ribosome protected footprints or total mRNA fragments

tif3Δ (FJZ052) and WT (FJZ046) strains growing exponentially in SC medium at 30°C were harvested by centrifugation at room temperature (R.T.) and resuspended in SC medium at 37°C or 15°C and incubated for 1h (37°C) or 10min (15°C) before treatment with 100ug/mL cycloheximide for 2min. Cells were harvested by vacuum filtration at R.T. and quick-frozen in liquid nitrogen. Cells were lysed in a freezer mill with lysis buffer buffer (20 mM Tris [pH 8.0], 140 mM KCl, 1.5 mM $MgCl_2$, 1% Triton, 100 µg/mL cycloheximide). For ribosome footprint library preparation, 30 A_{260} units of extract were treated with 450U of RNAse I (Ambion, #AM2295) for 1h at R.T. on a nutator, and ribosomes were pelleted by centrifugation on a 1M sucrose cushion. Ribosome-protected mRNA fragments (footprints) were purified using a miRNeasy Mini kit (Qiagen) per the vendor's instructions. Following size selection and dephosphorylation, a Universal miRNA cloning linker (New England Biolabs, #S1315S) was ligated to the 3' ends of footprints, followed by reverse transcription, circular ligation, rRNA subtraction, PCR amplification of the cDNA library, and DNA sequencing with an Illumina

HiSeq system. For RNA-seq library preparation, total RNA was purified using miRNeasy Mini kit (Qiagen) from aliquots of the same extracts used for footprint library preparation. Polyadenylated mRNA was isolated from total RNA using the Poly(A)Purist MAG Kit (Ambion #AM1922), and randomly fragmented at 70^{o}C for 8min in fragmentation reagent (Ambion #AM8740). Fragment size selection, library generation and sequencing were carried out as above. Ribosome footprint and RNA-seq libraries were prepared and sequenced from 2 independent cultures (biological replicates) for each pair of WT and mutant strains under comparison.

Linker sequences were trimmed from Illumina reads and the trimmed fasta sequences were aligned to the *S. cerevisiae* ribosomal database using Bowtie (3). The non-rRNA reads (unaligned reads) were then mapped to the *S. cerevisiae* genome using TopHat (4). Only uniquely mapped reads from the final genomic alignment were used for subsequent analyses (5).

Table S1. Plasmids used in this study

Plasmid	Description	Source/Reference
FLUC reporter plasmids containing native promoter, 5'UTR and first 20 codons of the indicated genes		
pNDS16	*YDL145C* in pRS416	(1)
pNDS19	*YPR159W* in pRS416	(1)
pNDS23	*YLR378C* in pRS416	(1)
pNDS26	*YKL004W* in pRS416	(1)
pNDS29	*YGL008C* in pRS416	(1)
pNDS37	*YHR071W* in pRS416	(1)
pFJZ872	*YML128C* in pRS416	(1)
pFJZ873	*YHL016C* in pRS416	(1)
Full-length and truncated FLUC reporters with $(CAA)_n$ repeats and SL insertions in a modified RPL41A 5'UTR		
pFJZ526	*FLUC* reporter with 70nt synthetic 5'UTR with $(CAA)_n$ repeats in YCplac33	This study
pFJZ683	*FLUC* reporter with cap-proximal SL with ΔG of -10.5 kcal/mol in synthetic 5'UTR in YCplac33	This study
pFJZ685	*FLUC* reporter with cap-proximal SL with ΔG of -5.7 kcal/mol in synthetic 5'UTR in YCplac33	This study
pFJZ688	*FLUC* reporter with cap-distal SL with ΔG of -10.5 kcal/mol in synthetic 5'UTR in YCplac33	This study
pFJZ690	*FLUC* reporter with cap-distal SL with ΔG of -5.7 kcal/mol in synthetic 5'UTR in YCplac33	This study
pFJZ538	Truncated *FLUC* reporter with 70nt synthetic 5'UTR with $(CAA)_n$ repeats in YCplac33	This study
pFJZ541	Truncated *FLUC* reporter with cap-proximal SL with ΔG of -10.5 kcal/mol in synthetic 5'UTR in YCplac33	This study

SUPPLEMENTAL REFERENCES

1. Sen ND, Zhou F, Ingolia NT, & Hinnebusch AG (2015) Genome-wide analysis of translational efficiency reveals distinct but overlapping functions of yeast DEAD-box RNA helicases Ded1 and eIF4A. *Genome Res* 25(8):1196-1205.
2. Chiu WL*, et al.* (2010) The C-terminal region of eukaryotic translation initiation factor 3a (eIF3a) promotes mRNA recruitment, scanning, and, together with eIF3j and the eIF3b RNA recognition motif, selection of AUG start codons. *Mol Cell Biol* 30(18):4415-4434.
3. Langmead B, Trapnell C, Pop M, & Salzberg SL (2009) Ultrafast and memory-efficient alignment of short DNA sequences to the human genome. *Genome Biol* 10(3):R25.
4. Trapnell C, Pachter L, & Salzberg SL (2009) TopHat: discovering splice junctions with RNA-Seq. *Bioinformatics* 25(9):1105-1111.
5. Ingolia NT, Ghaemmaghami S, Newman JR, & Weissman JS (2009) Genome-wide analysis in vivo of translation with nucleotide resolution using ribosome profiling. *Science* 324(5924):218-223.
6. Kertesz M*, et al.* (2010) Genome-wide measurement of RNA secondary structure in yeast. *Nature* 467(7311):103-107.
7. Park EH, Zhang F, Warringer J, Sunnerhagen P, & Hinnebusch AG (2011) Depletion of eIF4G from yeast cells narrows the range of translational efficiencies genome-wide. *BMC Genomics* 12(1):1-18.

Additional file 1. Excel file containing results of ribosome profiling of WT and *tif3Δ* cells at 37°C or 15°C. Spreadsheet 1, "*tif3(37)*_all expression", tabulates $\log_2$ values of the following parameters for the 5330 expressed genes listed in columns A-B for WT and *tif3*Δ cells at 37°C: Ribosome footprint sequencing reads (ribo_WT and ribo_*tif3Δ*); mRNA sequencing reads (mrna_WT and mrna_*tif3Δ*); the ratios ribo_*tif3Δ*/ribo_WT ($\Delta ribo_{tif3\Delta(37)}$) and mrna_*tif3Δ*/mrna_WT ($\Delta mRNA_{tif3\Delta(37)}$); and the ratio $\Delta ribo_{tif3\Delta}/\Delta mRNA_{tif3\Delta}$ ($\Delta TE_{tif3\Delta(37)}$);. Spreadsheet 2, "eIF4B hyperdependent genes", tabulates 159 genes exhibiting $\Delta TE_{tif3\Delta(37)} \leq 0.5$ or $\Delta TE_{tif3\Delta(37)} \geq 2.0$, with the $\log_2(\Delta TE_{tif3\Delta(37)})$ values listed in column C. Spreadsheet 3, "genome wide PARS dataset", contains PARS scores for the indicated features of the 5'UTR or CDS (see text of RESULTS for definitions of all features) for the 2679 genes (listed in column A) whose PARS scores were compiled by (6). Spreadsheet 4, "PARS_eIF4B hyperdependent genes", contains PARS scores for the indicated 5'UTR or CDS features for the 72 genes exhibiting $\Delta TE_{tif3\Delta(37)} \leq 0.5$ or $\Delta TE_{tif3\Delta(37)} \geq 2.0$ (from Spreadsheet 2) whose PARS scores were compiled by (6). Spreadsheet 5, " *tif3(15)*_all expression", tabulates $\log_2$ values of the parameters indicated in the legend of additional file 1 for the 5190 expressed genes listed in columns A-B for WT and *tif3*Δ cells at 15°C. Spreadsheet 6 "eIF4B hyperdependent genes (15)" tabulates 166 genes exhibiting $\Delta TE_{tif3\Delta(15)} \leq 0.5$ or $\Delta TE_{tif3\Delta(15)} \geq 2.0$, with the $\log_2(\Delta TE_{tif3\Delta(15)})$ values listed in column B.

Fig.S1

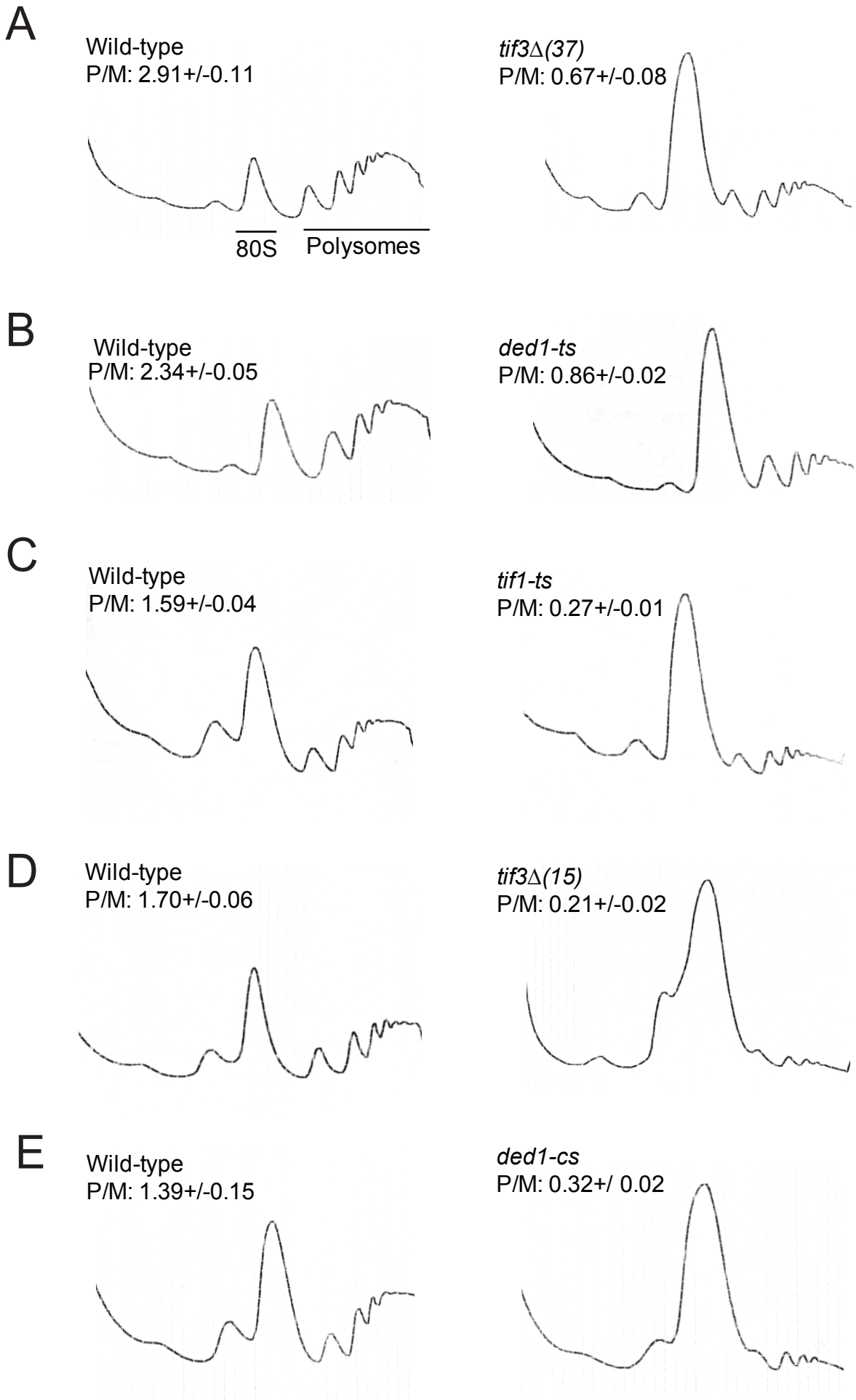
A
Wild-type
P/M: 2.91+/-0.11
80S
Polysomes
tif3Δ(37)
P/M: 0.67+/-0.08
B
Wild-type
P/M: 2.34+/-0.05
ded1-ts
P/M: 0.86+/-0.02
C
Wild-type
P/M: 1.59+/-0.04
tif1-ts
P/M: 0.27+/-0.01
D
Wild-type
P/M: 1.70+/-0.06
tif3Δ(15)
P/M: 0.21+/-0.02
E
Wild-type
P/M: 1.39+/-0.15
ded1-cs
P/M: 0.32+/ 0.02

Figure S1. *tif3, ded1* and *tif1* mutations substantially impair polysome assembly in vivo.

(A-E) Cells growing exponentially at 30°C in SC, SC-Leu, or SC-His medium, as indicated below, were collected by centrifugation at room temperature (RT), resuspended in the same pre-cooled or pre-warmed medium, and incubated as follows: **(A)** FJZ046 (WT) and FJZ052 (*tif3Δ*) in SC at 37°C for 1h; **(B)** NSY10 (WT) and NSY11 (*ded1-ts*) in SC-His at 37°C for 2h; **(C)** NSY20 (WT) and NSY21(*tif1-ts*) in SC-Leu at 37°C for 1h; **(D)** FJZ046 (WT) and FJZ052 (*tif3Δ*) in SC at 15°C for 10 min; **(E)** NSY4 (WT) and NSY5 (*ded1-cs*) in SC-Leu at 15°C for 10 min. Following treatment with cycloheximide, WCEs were resolved by sedimentation through sucrose gradients, and gradients were scanned at 254 nm to yield the indicated tracings. Average polysome/monosome ratios (P/M) from three biological replicates are shown, as means +/- S.E.M. Panels B,C and E are reproduced from (1) for comparison to results in panels A & D.

Fig. S2

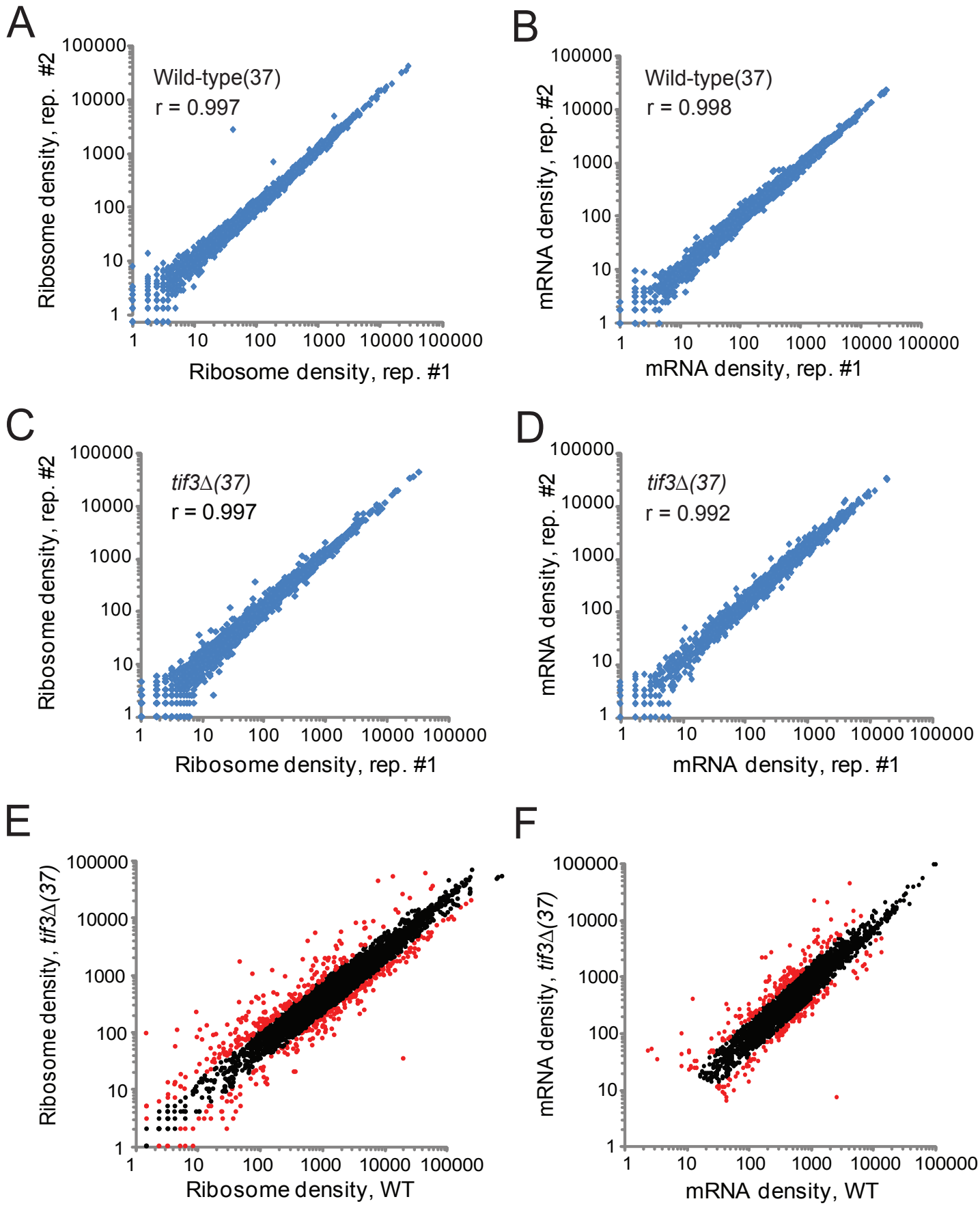
A
Wild-type(37)
r = 0.997
Ribosome density, rep. #2
Ribosome density, rep. #1
B
Wild-type(37)
r = 0.998
mRNA density, rep. #2
mRNA density, rep. #1
C
tif3Δ(37)
r = 0.997
Ribosome density, rep. #2
Ribosome density, rep. #1
D
tif3Δ(37)
r = 0.992
mRNA density, rep. #2
mRNA density, rep. #1
E
Ribosome density, tif3Δ(37)
Ribosome density, WT
F
mRNA density, tif3Δ(37)
mRNA density, WT
1
10
100
1000
10000
100000

Figure S2. Genome-wide ribosome footprint and mRNA reads for WT and *tif3Δ* strains at 37°C.

(A–D) Scatterplots of ribosome footprint and RNA-seq reads of biological replicates of WT and *tif3Δ* strains. Pearson correlation coefficients (r) were calculated for genes with >128 total mRNA reads in the 4 samples combined (two strains and their two replicates). **(E-F)** Scatterplots of normalized read densities expressed as number of reads mapping to gene coding sequences normalized by coding sequence length and total number of reads for that sample. (E) ribosome footprint read density and (F) mRNA read density for *tif3Δ* versus WT cells following a shift from 30°C to 37°C for 1h.

Fig. S3

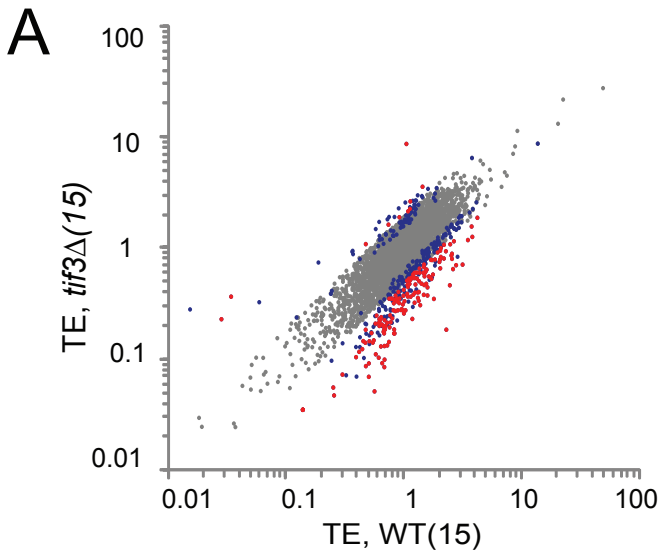
A
100
10
1
0.1
0.01
TE, tif3Δ(15)
0.01
0.1
1
10
100
TE, WT(15)

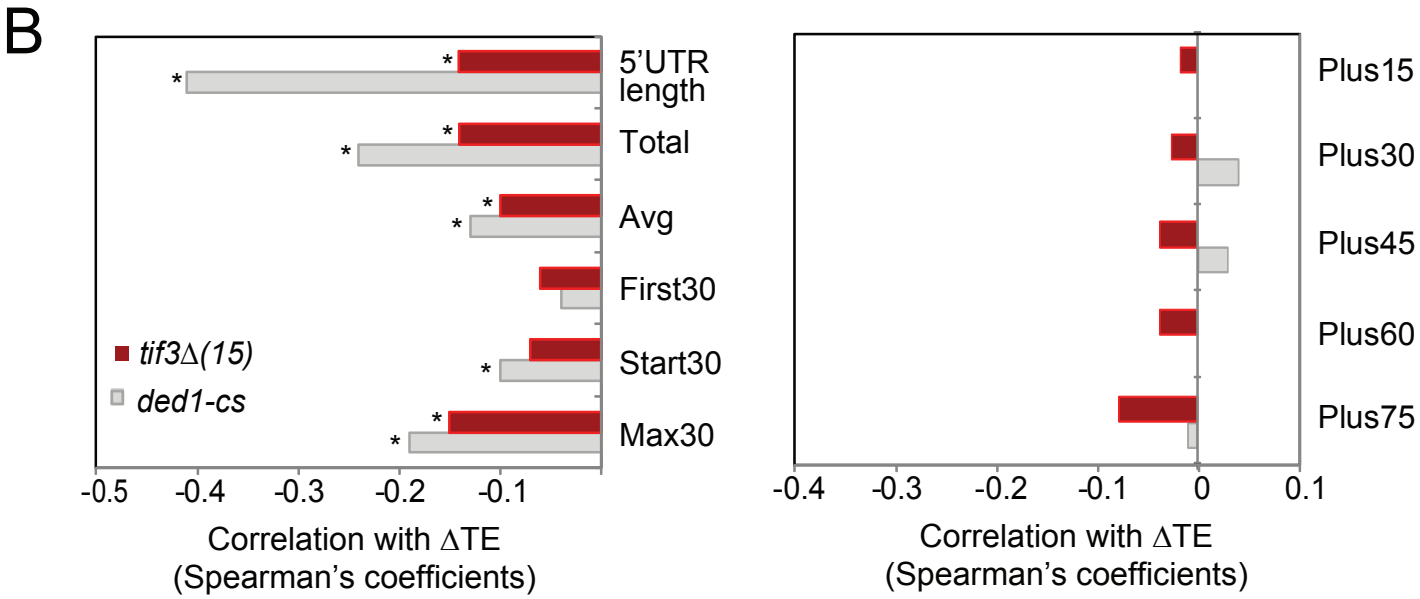
B
5'UTR length
Total
Avg
First30
Start30
Max30
tif3Δ(15)
ded1-cs
-0.5
-0.4
-0.3
-0.2
-0.1
Correlation with ΔTE
(Spearman's coefficients)
Plus15
Plus30
Plus45
Plus60
Plus75
-0.4
-0.3
-0.2
-0.1
0
0.1
Correlation with ΔTE
(Spearman's coefficients)

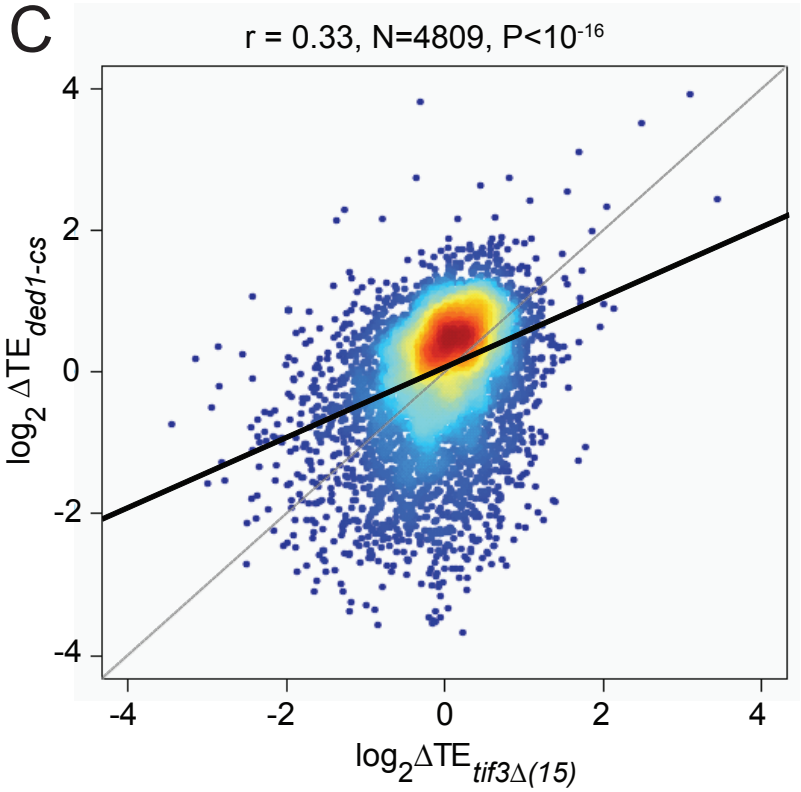
C
r = 0.33, N=4809, P<10-16
4
2
0
-2
-4
log2 ΔTEded1-cs
-4
-2
0
2
4
log2ΔTEtif3Δ(15)

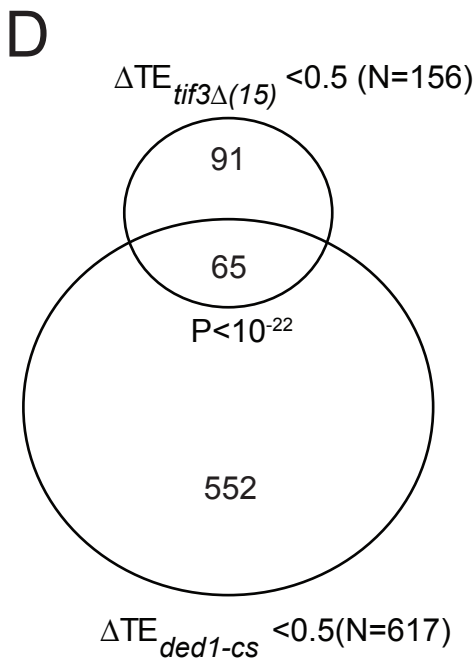
D
ΔTEtif3Δ(15) <0.5 (N=156)
91
65
P<10-22
552
ΔTEded1-cs <0.5(N=617)

Figure S3. Correlation between genome-wide changes in relative TE conferred by elimination of eIF4B or inactivation of Ded1 at 15°C.

(A) Scatterplot of TEs in *tif3Δ* versus WT cells at 15°C, as in Fig. 1A. Genes exhibiting twofold or greater changes in *tif3Δ* cells at FDR<0.01 or >1.4-fold changes at FDR<0.05 are highlighted in red and blue, respectively**. (B)** Spearman coefficients from correlations between ΔTE values conferred by the indicated mutations and 5'UTR lengths or the indicated cumulative PARS scores, for all 2607 genes, curated by Kertesz et al (2010) (*, $P<10^{-16}$). Published ΔTE values for *ded1-cs* mutants were employed (1). **(C)** Density plot of $\log_2$ΔTE values for 4811 expressed genes for *ded1-cs* versus *tif3Δ* cells at 15°C, strains, using *ded1-cs* data from (1), generated as in Fig. 1D **(D)** Overlap between eIF4B- and Ded1-hyperdependent genes exhibiting ≥2-fold reductions in TE at 15°C in *tif3Δ* and *ded1-cs* strains.

Fig. S4

A

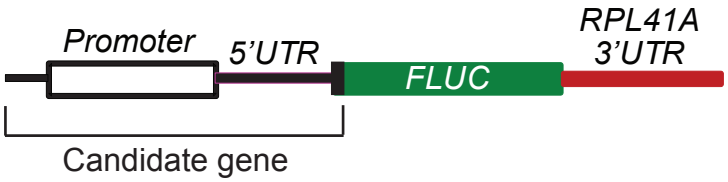

B

ORF	Luciferase Expression (*tif3*Δ/WT)	Δribo$_{tif3\Delta(37)}$	ΔmRNA$_{tif3\Delta(37)}$	ΔTE$_{tif3\Delta(37)}$
YHR071W/*PCL5*	0.13 +/- 0.02	0.18	0.87	0.20
YML128C/MSC1	0.29 +/- 0.04	0.37	0.78	0.48
YHL016C/DUR3	0.26 +/- 0.06	0.39	0.94	0.42
YKL004W/AUR1	0.60 +/- 0.08	0.44	0.76	0.58
YPR159W/KRE6	0.87 +/- 0.09	0.57	0.89	0.64
YGL008C/PMA1	0.53 +/- 0.04	0.6	0.99	0.61
YDL145C/COP1	0.87 +/- 0.09	0.68	1.17	0.58
YLR378C/SEC61	0.66 +/- 0.09	0.73	1.14	0.64

C

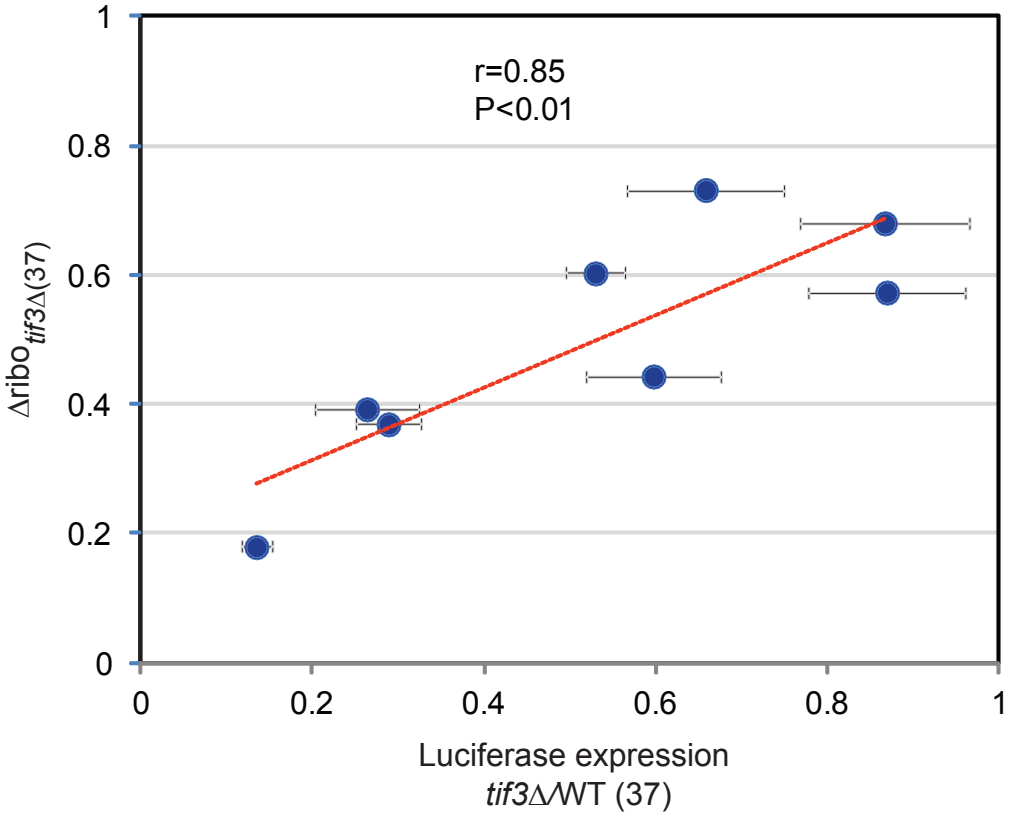

Figure S4. Identification of 5'UTRs that confer eIF4B-dependence of *LUC* reporter expression.

(A) Schematic representation of the gene-specific inserts, comprising the promoter, 5′ UTR and first 20 codons, fused to the coding sequences of firefly luciferase (*FLUC*) and a modified 3'UTR of yeast *RPL41A,* for 8 different yeast genes. **(B)** Comparison between changes in *LUC* reporter expression and ribosome density in the *tif3*Δ mutant versus WT cells at 37°C for eight candidate genes. Luciferase expression ratios (*tif3*Δ/WT) were determined for *LUC* reporters containing the promoter, 5'UTR, and first 20 codons of the corresponding genes in column 1, as described in (A). The $\Delta ribo_{tif3\Delta(37)}$, $\Delta mRNA_{tif3\Delta(37)}$ and $\Delta TE_{tif3\Delta(37)}$ values determined by ribosome footprint profiling and RNA-Seq analysis of *tif3Δ* and WT cells at 37°C were extracted from Additional File 1. **(C)** Changes in ribosome density of the 8 genes (from ribosome footprints) in *tif3Δ* versus WT cells at 37°C plotted against the ratio of luciferase expression in *tif3Δ* versus WT cells for the corresponding reporters. Strains WT (FJZ046) and *tif3Δ* (FJZ052) harboring *LUC* reporter plasmids were grown in SC-Ura at 30°C, diluted to OD_{600}~0.1, and grown for ~3 doublings at 37°C (~18h for *tif3Δ* and ~6h for WT). Luciferase activities were assayed in WCEs, normalized to total protein, and reported in relative light units (RLUs) per mg of protein. Means (+/- S.E.M.) determined from 6 independent transformants are plotted.

A

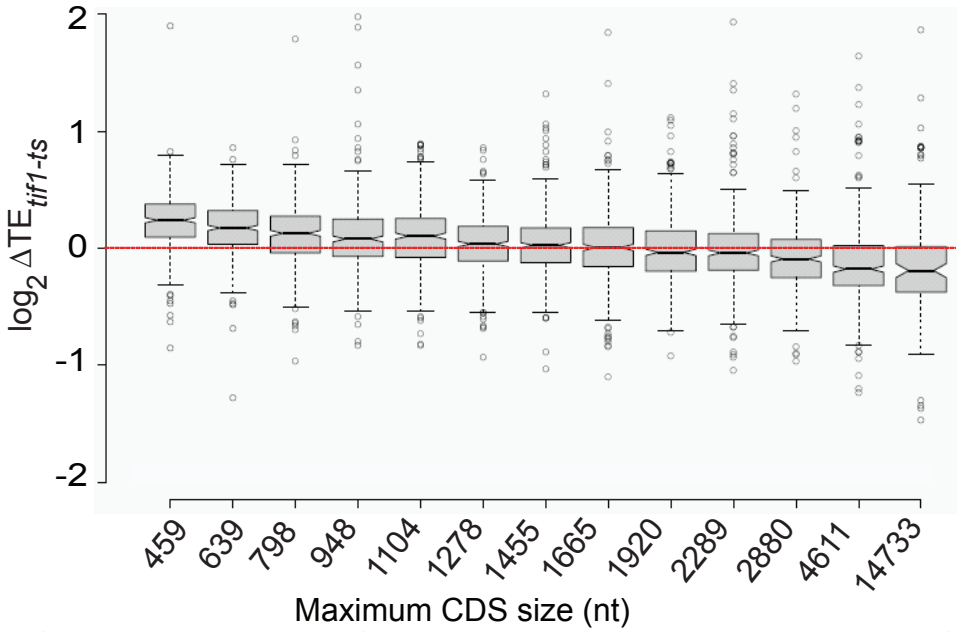

Fig. S5

B

mRNA feature	Correlations of $\Delta TE_{tif3\Delta(37)}$ with mRNA feature (ρ)	Correlations of residuals from Loess regression of $\Delta TE_{tif3\Delta(37)}$ against mRNA feature (ρ)		
		Residuals ΔTE vs. CDS length	Residuals ΔTE vs. 5'UTR length	Residuals ΔTE vs. Total PARS
CDS length	-0.76	0.03	-0.7	-0.73
5'UTR length	-0.3	-0.13	0.01	-0.22
Total PARS	-0.23	-0.12	-0.15	-0.01
P value: N=2382	$< e^{-12}$	$< e^{-8}$		

Figure S5. Longer mRNAs tend to have heightened dependence on Ded1 and eIF4A while shorter mRNAs are unusually dependent on eIF4G.

(A) Notched box-plot of ΔTE values in the *tif1-ts* mutant versus WT cells for bins of 400 genes arranged by increasing CDS length, as in Fig. 6B except that the last bin contains 107 genes, constructed using published data (1). **(B)** LOESS regression analysis of $\Delta TE_{tif3\Delta(37)}$ against CDS length, 5'UTR length, Total PARS was conducted using the loess function from the R 'stats' library and the residuals from each regression were correlated with CDS length, 5'UTR length, or Total PARS, resulting in the Spearman's coefficients tabulated in columns 3-5, respectively. Column 2 reproduces the Spearman's coefficients determined in Fig. 5A for comparison purposes.

Fig. S6

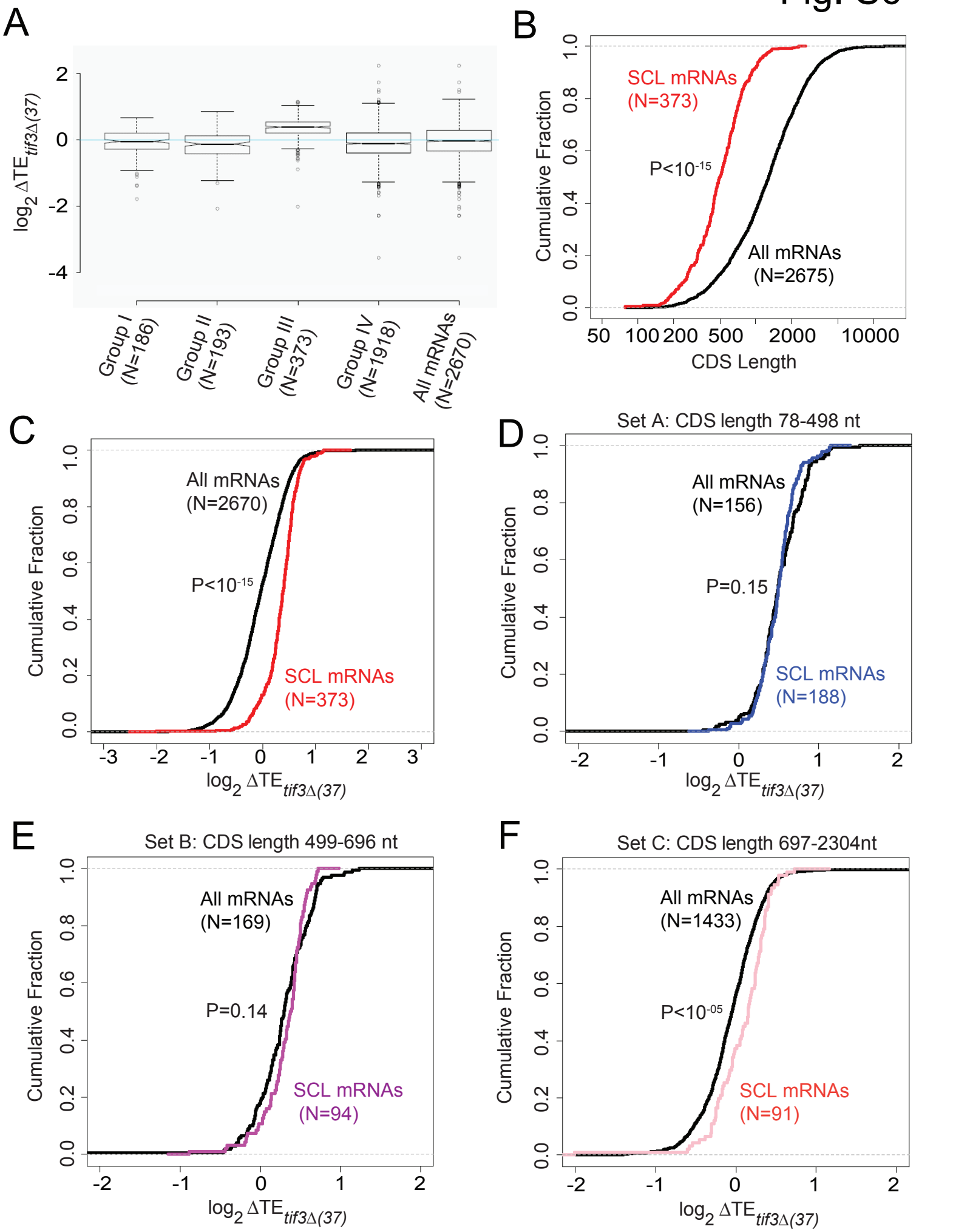
A
log2 ΔTE tif3Δ(37)
2
0
-2
-4
Group I (N=186)
Group II (N=193)
Group III (N=373)
Group IV (N=1918)
All mRNAs (N=2670)
B
Cumulative Fraction
SCL mRNAs (N=373)
P<10-15
All mRNAs (N=2675)
CDS Length
50 100 200 500 2000 10000
C
All mRNAs (N=2670)
P<10-15
SCL mRNAs (N=373)
log2 ΔTE tif3Δ(37)
D
Set A: CDS length 78-498 nt
All mRNAs (N=156)
P=0.15
SCL mRNAs (N=188)
E
Set B: CDS length 499-696 nt
All mRNAs (N=169)
P=0.14
SCL mRNAs (N=94)
F
Set C: CDS length 697-2304nt
All mRNAs (N=1433)
P<10-05
SCL mRNAs (N=91)

Figure S6. Longer mRNAs with a low potential for closed-loop formation have a heightened requirement for eIF4B.

(A) Notched box-plots of ΔTE values in the *tif3Δ* mutant versus WT cells at 37°C for four different groups of genes described in Costello et al. (2015) that vary in mRNA-occupancies by proteins that promote or oppose closed-loop formation. The strong closed-loop (SCL) forming mRNAs in Group III are translated relatively better, whereas mRNAs in Groups I, II and IV are translated relatively worse in cells lacking eIF4B. **(B)** Cumulative distributions of CDS lengths for the SCL group of mRNAs, and all mRNAs, analysed by Costello et al, with the P-value indicated for a Kolmogorov–Smirnov test indicating that SCL mRNAs have significantly smaller CDS lengths versus all mRNAs. **(C)** Fig 7C reproduced here for comparison. **(D-F)** Cumulative distributions of ΔTE values in the *tif3Δ* mutant versus WT cells at 37°C for three subsets of the SCL mRNAs divided on the basis of CDS length, as indicated above each graph. The CDS lengths defining each subset were chosen arbitrarily to achieve a sufficient number of genes in each subset (~90 or more) for statistical analysis. Each subset of SCL mRNAs was compared to a length-matched subset of all other mRNAs analysed by Costello et al after excluding the SCL transcripts. P-values of Kolmogorov–Smirnov test of statistical significance of the differences between the two cumulative distributions are indicated.

It might seem surprising that 282 of the 373 SCL mRNAs (~75%) of short and intermediate CDS lengths (Sets A and B) closely resemble their non-SCL counterparts in response to eliminating eIF4B (panels D-E), whereas the entire SCL group is significantly less sensitive than all other mRNAs to the absence of eIF4B (panel C). This follows from the fact that Sets A and B of the SCL group are being compared to the relatively small fractions (~6 % each) of all remaining

mRNAs with comparable CDS lengths in panels D-E, whereas the SCL group was compared to all mRNAs in panel C, most of which have CDS lengths >696nt.

Fig. S7

A

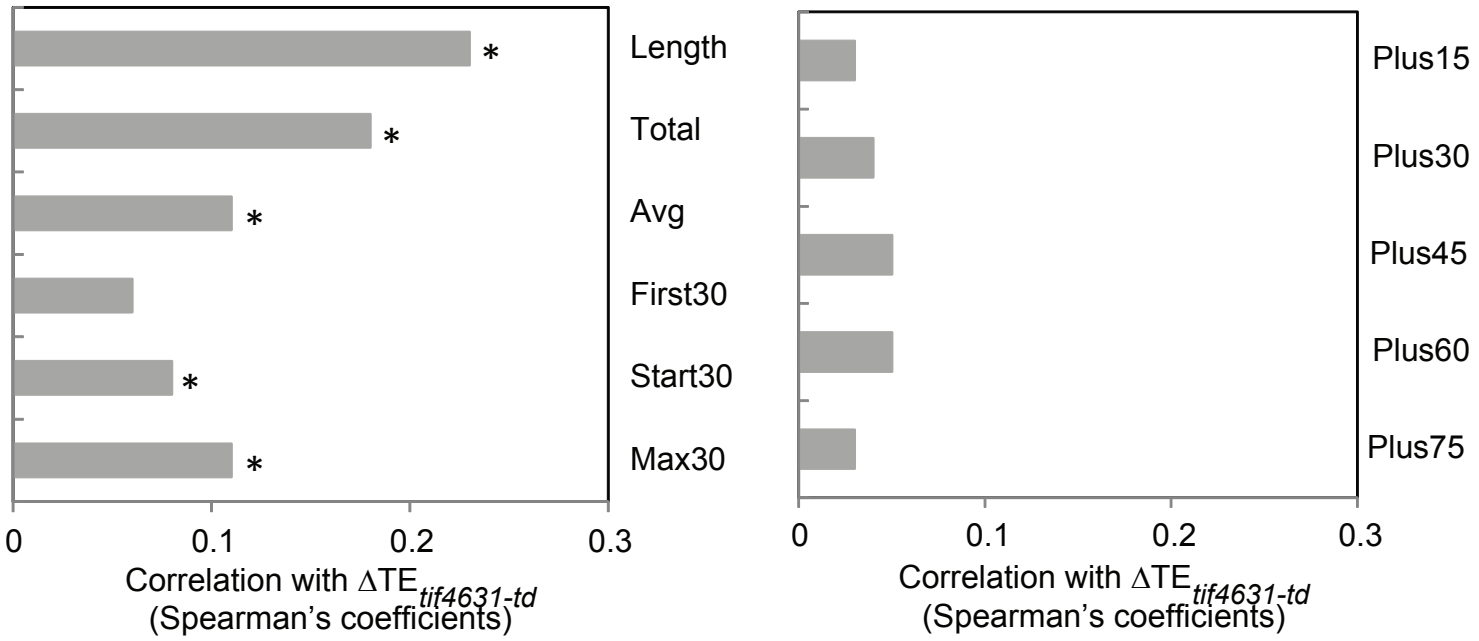
Length
Total
Avg
First30
Start30
Max30
*
0
0.1
0.2
0.3
Correlation with ΔTE tif4631-td
(Spearman's coefficients)
Plus15
Plus30
Plus45
Plus60
Plus75

B

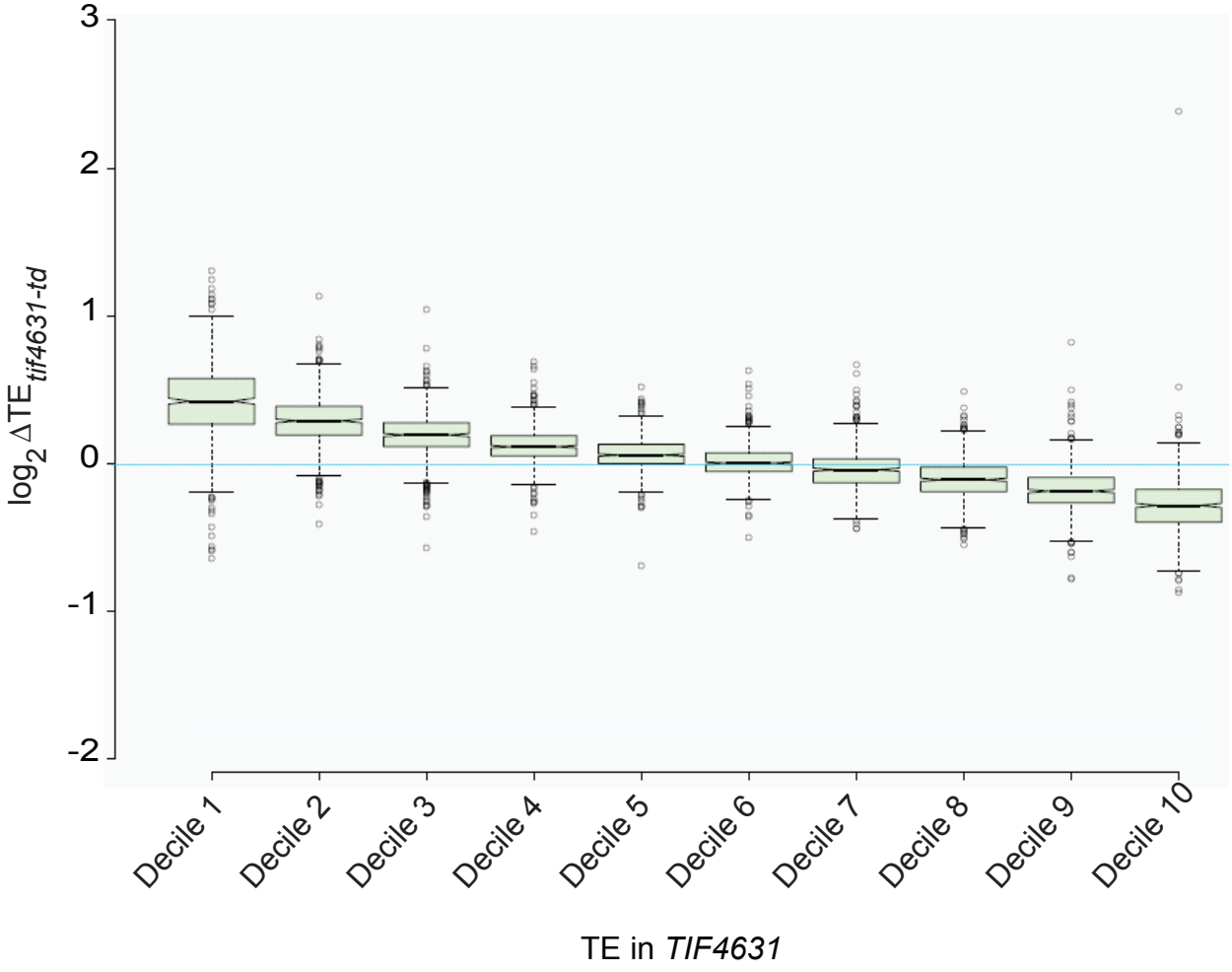
log2 ΔTE tif4631-td
3
2
1
0
-1
-2
Decile 1
Decile 2
Decile 3
Decile 4
Decile 5
Decile 6
Decile 7
Decile 8
Decile 9
Decile 10
TE in TIF4631

Figure S7. mRNAs with a heightened dependence on eIF4G for efficient translation tend to short and contain short, unstructured 5'UTRs.

(A) Spearman coefficients from correlations between ΔTE values in the *tif4631-td* mutant versus WT cells and the 5'UTR length or PARS features described in Fig. 4A (*, $P<10^{-16}$). (B) Notched box-plots of ΔTE values in the *tif4631-td* mutant versus WT cells in deciles of genes arranged by increasing TE in WT cells. Published TEs in WT and ΔTE values in the *tif4631-td* mutant were employed (7).

Fig. S8

Constructs for cross-linking assays

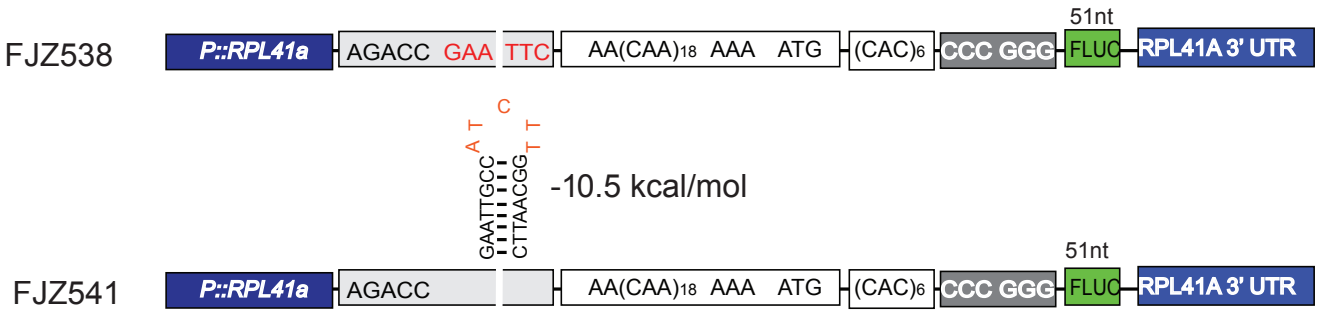

Constructs for luciferase assays

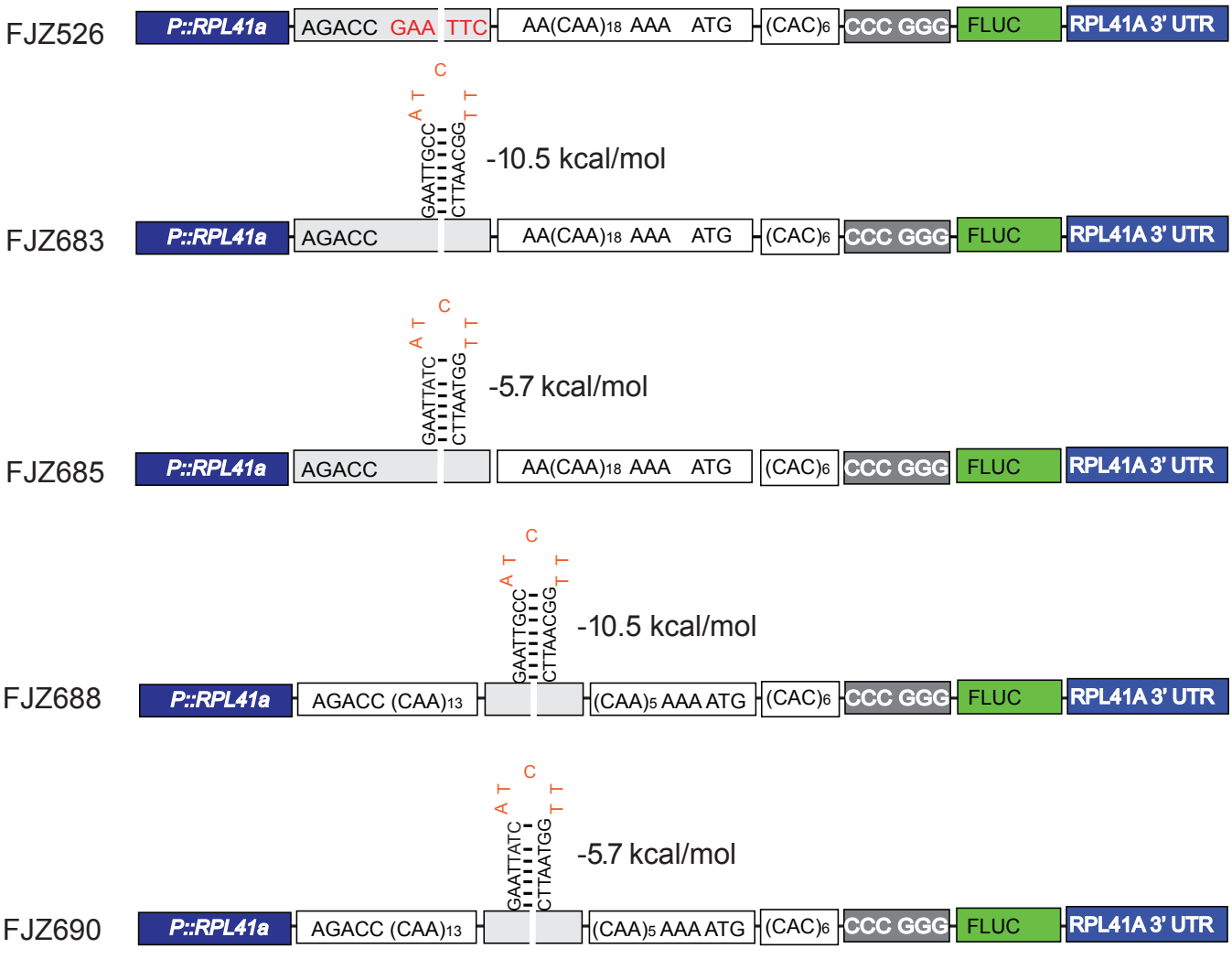

Figure S8. Full-length and truncated *LUC* reporters harboring unstructured 5'UTRs with and without SL insertions

Schematic depiction of 5'UTR sequences of reporter genes analyzed in Fig. 5A-B. See Supplemental Materials for details on their construction.